Cellular and Molecular Mechanisms of Arrhythmias in Cardiac Fibrosis and Beyond:

From Symptoms to Substrates towards Solutions

Chapter IV

Similar Arrhythmicity in Hypertrophic and Fibrotic Cardiac Cultures Caused by Distinct Substrate-Specific Mechanisms

Substrate-Dependent Arrhythmic Mechanisms

Saïd F. A. Askar, MSc*; Brian O. Bingen, MD*; Martin J. Schalij, MD, PhD; Jim Swildens, Msc; Douwe E. Atsma, MD, PhD; Cindy I. Schutte, BSc; Antoine A. F. de Vries, PhD; Katja Zeppenfeld, MD, PhD; Dirk L. Ypey, PhD; Daniël A. Pijnappels, PhD.

*Equal contribution

Adapted from Cardiovasc Res 2013;97:171-181

Abstract

Aims: Cardiac hypertrophy and fibrosis are associated with potentially lethal arrhythmias. As these substrates often occur simultaneously in one patient, distinguishing between pro-arrhythmic mechanisms is difficult. This hampers understanding of underlying pro-arrhythmic mechanisms and optimal treatment. This study investigates and compares arrhythmogeneity and underlying pro-arrhythmic mechanisms of either cardiac hypertrophy or fibrosis in *in vitro* models.

Methods & Results: Fibrosis was mimicked by free myofibroblast (MFB) proliferation in neonatal rat ventricular monolayers. Cultures with inhibited MFB proliferation were used as control or exposed to phenylephrine to induce hypertrophy. At day 9, cultures were studied with patch-clamp and optical-mapping techniques and assessed for protein expression. In hypertrophic (n=111) and fibrotic cultures (n=107), conduction and repolarization were slowed. Triggered activity was commonly found in these substrates and led to high incidences of spontaneous reentrant arrhythmias (67.5% hypertrophic, 78.5% fibrotic vs. 2.9% in controls (n=102)) or focal arrhythmias (39.1% 51.7% vs. 8.8% respectively). Kv4.3 and Cx43 protein expression levels were decreased in hypertrophy but unaffected in fibrosis. Depolarization of cardiomyocytes (CMCs) was only found in fibrotic cultures (-48±7mV vs. -66±7mV in control, $P<0.001$). L-type calcium-channel blockade prevented arrhythmias in hypertrophy, but caused conduction block in fibrosis. Targeting heterocellular coupling by low doses of gap-junction uncouplers prevented arrhythmias by accelerating repolarization only in fibrotic cultures.

Conclusions: Cultured hypertrophic or fibrotic myocardial tissues generated similar focal and reentrant arrhythmias. These models revealed electrical remodeling of CMCs as a pro-arrhythmic mechanism of hypertrophy and MFB-induced depolarization of CMCs as a pro-arrhythmic mechanism of fibrosis. These findings provide novel mechanistic insight into substrate-specific arrhythmicity.

Introduction

Pathophysiological alterations in myocardial structure as observed in cardiac fibrosis or hypertrophy are associated with the occurrence of lethal cardiac arrhythmias.[1-3] As hypertrophy and fibrosis may occur concomitantly to varying degrees in cardiac remodeling in one patient, it remains unclear how these adaptations independently contribute to the arrhythmogeneity of remodeled tissue. Hence, the mechanisms through which hypertrophy or fibrosis cause arrhythmias remain incompletely understood. Because hypertrophy and fibrosis are characterized by specific modifications at molecular and cellular levels, these alterations could thereby provide a basis for distinct substrate-specific pro-arrhythmic mechanisms. Although treatment of cardiac arrhythmias has improved over recent years, it remains suboptimal in terms of efficacy and safety.[4-6] The notion that pharmacological anti-arrhythmic treatment does not significantly improve survival, and may in fact evoke lethal arrhythmias, could indicate that anti-arrhythmic treatment, without detailed knowledge of the underlying pro-arrhythmic mechanisms, may limit therapeutic efficacy.[7] Therefore, this study aimed to identify and compare independent mechanisms of arrhythmias in hypertrophic or fibrotic myocardial tissue and thereby determine the arrhythmogeneity per substrate. The results revealed a similar occurrence of prolongation of repolarization, triggered activity and reentrant tachyarrhythmias in fibrotic and hypertrophic myocardial cultures. However, the underlying pro-arrhythmic mechanisms in these substrates were distinct, being of intrinsic nature in cardiac hypertrophy and of extrinsic origin in cardiac fibrosis.

Materials and Methods

All animal experiments were approved by the Animal Experiments Committee of the Leiden University Medical Center and conform to the Guide for the Care and Use of Laboratory Animals as stated by the US National Institutes of Health.

Cell Isolation and culture

Isolation of primary neonatal rat ventricular myocardial cells was performed as described previously.[8] In brief, animals were anaesthetized with 4–5% isoflurane inhalation anaesthesia. Adequate anaesthesia was assured by the absence of reflexes prior to rapid heart excision. After animal sacrifice by rapid heart excision, ventricular tissue was minced and digested with collagenase I (450 units/ml; Worthington, NJ, USA) in two digestion steps of 50 and 40 minutes. After a 75-minute pre-plating step to minimize the amount of fibroblasts in cardiac cell preparation, cells were plated out on fibronectin-coated, round glass coverslips (15 mm) at a cell density of 1-8x10^5 cells/well in 24-well plates (Corning Life Sciences, Amsterdam, the Netherlands) depending on the experiment. To mimic fibrosis, endogenously present myofibroblasts (MFBs) proliferated freely. As control, proliferation was inhibited by 10 µg/mL Mitomycin-C (Sigma-Aldrich, St. Louis, MO, USA) at day 1.[9] To induce hypertrophy, control cultures were exposed to 100 µM phenylephrine (PE, Sigma) for 24h at day 3 and day 8.

Immunocytological analyses

Cultures were stained for several markers of interest after 20 minute fixation in 1% paraformaldehyde and permeabilization with 0.1% Triton X-100. Primary antibodies (1:200) and corresponding secondary Alexa fluor-conjugated antibodies (1:400, Invitrogen, Carlsbad, CA, USA) were incubated for 2 hours. Counterstaining of nuclei was performed with Hoechst 33342 (Invitrogen). Images of cultures were quantified using dedicated software (Image-Pro Plus, version 4.1.0.0, Media Cybernetics, Silver Spring, MD, USA).

Western Blot

Hypertrophic, fibrotic or control cultures were homogenized in RIPA-buffer containing 50 mmol/L Tris-HCl (pH 8.0), 150 mmol/L NaCl, 1% Triton X-100, 0.5% sodiumdeoxycholate and 0.1% SDS. Then, 10 µg of protein per sample (at least 3 samples per group) were size-fractionated on NuPage 12% gels (Invitrogen) and transferred to Hybond PVDF membranes (GE Healthcare, Diegem, Belgium). Membranes were blocked in TBS-Tween (0.1%) + 5% Bovine Serum Albumin (Sigma) for 1h. Afterwards, these membranes were incubated with primary antibodies directed against Nav1.5 (Abcam, Cambridge, UK), Cav1.2, Kv4.3, Kir2.1, Kv7.1 (all from Alomone Labs, Jerusalem, Israel) for 1h, rinsed three times in TBS-Tween and then incubated with corresponding HRP-conjugated secondary antibodies (Santa Cruz Biotechnlogy, Santa Cruz, CA, USA) for 1h. Chemiluminescence was detected and caught on

hyperfilm ECL using ECL Prime detection reagents (GE Healthcare). To check for equal protein loading, GAPDH (Millipore, Billerica, MA, USA) expression was determined. To compare fibrotic and control groups, protein expression was subsequently adjusted for CMC content by normalizing for α-actinin (Sigma).

Optical mapping

Optical mapping in 24-well plates at a density of $8x10^5$ cells/well and subsequent analyses were performed as previously described.[9] At day 9, cultures were incubated with 8 μM Di-4-ANEPPS after which cultures were refreshed with DMEM/Hams F10 (37 °C) and optically mapped immediately using the Ultima-L mapping setup (SciMedia, Costa Mesa, CA, USA). Mapping experiments typically did not exceed 30 minutes per 24-wells plate. Also, cultures were not exposed to excitation light for longer than 50 s to limit possible phototoxic effects. Parameters of interest were determined using Brain Vision Analyze 1108 (Brainvision, Inc., Tokyo, Japan). The incidence of triggered activity was assessed in all groups after eliminating reentrant conduction by electrical stimulation. Triggered activity was defined as all newly formed optical action potentials independent of initial pacing- or spontaneous frequency, with >10% of the optical amplitude of the initial paced or spontaneous action potential. An early after depolarization (EAD) was defined as a reversal of repolarization during phase 2 or 3 of the action potential of > 10% of optical amplitude. Focal tachyarrhythmias were defined as non-reentrant activation patterns >3 repetitions faster than 2 Hz. Reentrant tachyarrhythmias were defined as repetitive circular activation patterns for >3 rotations at >2 Hz.

Pro-arrhythmic mechanisms studied by pharmacological interventions

Different pharmacological agents were administered during optical mapping for investigation of pro-arrhythmic mechanisms. To reduce the net inward current, L-type Ca^{2+} current was inhibited by administration of a relatively low dose of nitrendipine (3 μM) (Sigma) or verapamil (10 μM) (Centrafarm, Etten-Leur, the Netherlands) directly into the mapping medium. To reduce heterocellular coupling, a relatively low dose of 2-Amino-ethoxy diphenyl borate (2-APB, 5 μM) (Tocris Bioscience, Bristol, United Kingdom) or carbenoxolone (100 μM) (Sigma) was incubated for 20 minutes. To investigate effects of Nav1.5 blockade, tetrodotoxin (TTX, 20 μM, Alomone Labs) was directly used. For investigation of the involvement of intracellular calcium handling in arrhythmogeneity, intracellular calcium was buffered using 10-50 μM BAPTA-AM (Sigma) which incubated for 20 minutes. To investigate the effect of action potential duration (APD) prolongation on arrhythmogeneity, 0.5 mM sotalol (Sigma) was used. For reproducibility and comparability between all pharmacological interventions, all cultures were paced with a 1 Hz supra-threshold stimulation protocol during optical mapping recordings.

Whole-cell patch-clamp

Membrane potential recordings were performed with the whole-cell patch-clamp technique in hypertrophic cultures, co-cultures of cardiomyocytes (CMCs) and eGFP labeled MFBs at equal cell quantity and density as fibrotic cultures with freely proliferating MFBs, and control cultures. At day 9, after identification of CMCs by phase contrast and fluorescence microscopy, action potential properties were determined in current-clamp. Whole-cell recordings were performed at 25°C using a L/M-PC patch-clamp amplifier (3kHz filtering) (List-Medical, Darmstadt, Germany). The pipette solution contained (in mmol/L) 10 Na_2ATP, 115 KCl, 1 $MgCl_2$, 5 EGTA, 10 HEPES/KOH (pH 7.4). Tip and seal resistance were 2.0-2.5 MΩ and >1 GΩ, respectively. The bath solution contained (in mmol/L) 137 NaCl, 4 KCl, 1.8 $CaCl_2$, 1 $MgCl_2$, and 10 HEPES (pH 7.4). In a subset of experiments, CMCs were functionally uncoupled by incubation for 20 minutes with 25 µmol/L 2-APB to investigate action potential characteristics in hypertrophic, fibrotic or control cultures. For data acquisition and analysis, pClamp/Clampex8 software (Axon Instruments, Molecular Devices, Sunnyvale, CA, USA) was used.

Statistical analysis

Statistical analyses were performed using SPSS11.0 for Windows (SPSS, Inc., Chicago, IL, USA). Differences were considered statistically significant if $P<0.05$.

Results

Cellular characterization of hypertrophic myocardial cultures

In PE-treated cultures, expression levels of ANP (126.9±8.1 vs. 93.4±5.6 arbitrary units, $P<0.001$) (Supplemental figure 1A and 1B) and α-Skeletal Muscle Actin (131.0±9.0 vs. 116.5±17.0 arbitrary units, $P<0.01$) (Supplemental figure 1C and 1D) were significantly higher compared to control cultures. Furthermore, a significant increase from 1.4±0.7 10^6 pixels to 2.6±0.6x10^6 pixels ($P<0.05$) in cell surface area was observed (Supplemental figure 1F). Non-myocytes expressed α-Smooth-Muscle-Actin and Collagen-I as determined by immunocytological staining and were therefore considered MFBs. Moreover, cellular composition of cultures was analyzed by collagen I/α-actinin double staining, suitable for distinction between MFBs and CMCs.[9] Administration of PE to cardiac cultures did not influence MFB quantities (18.6±2.8% vs. 18.1±2.0% in control cultures, p=ns) (Supplemental figure 1E) or CMC quantities. As MFB quantities were as low as control cultures, PE-treated cultures were considered primarily pathologically hypertrophic with a minimal fibrotic component.

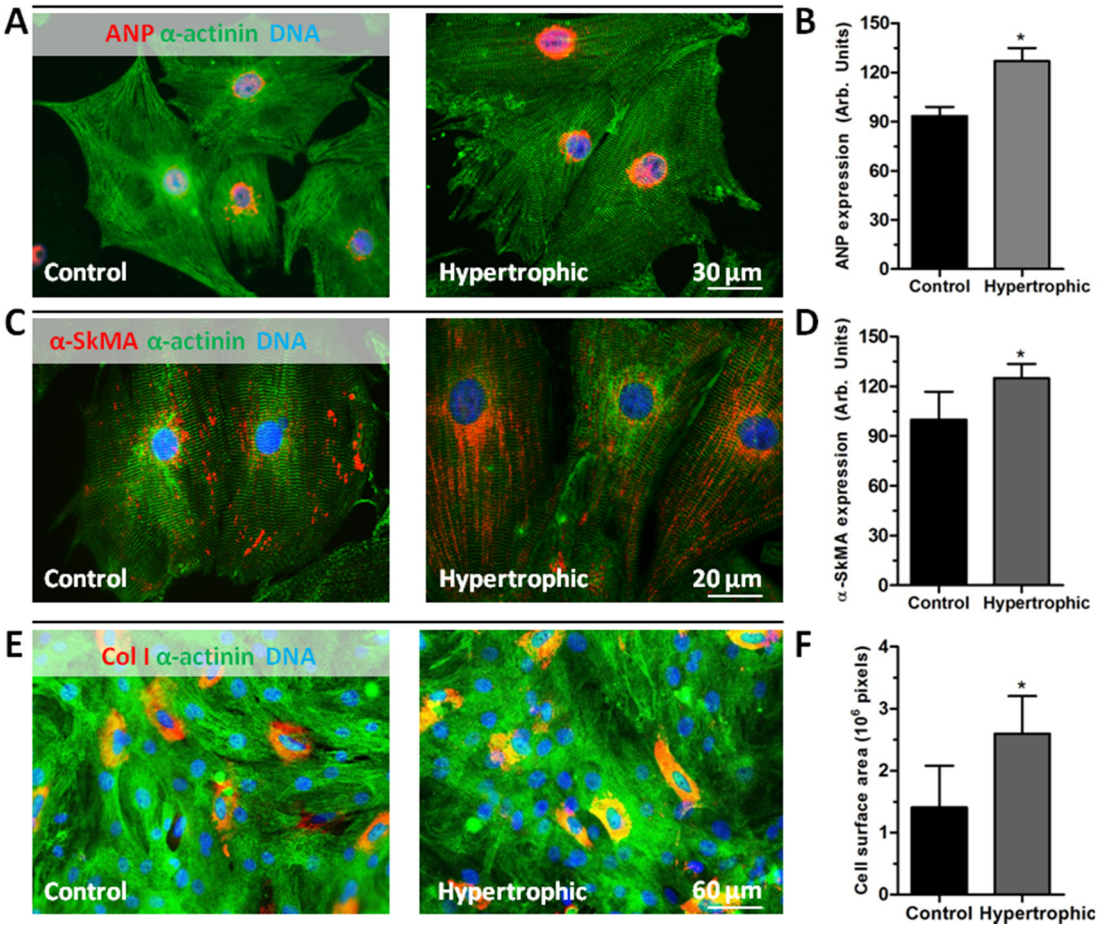

Supplemental Figure 1. *Cellular characterization of hypertrophic myocardial cultures. (A) Typical examples of immunocytological double-staining for ANP (red) and α-actinin (green). (B) Quantification of ANP signal. *:p<0.001 vs control. (C) Immunocytological double-staining for α-skeletal actin (red) and α-actinin (green). (D) Quantification of α-skeletal actin signal. *:p<0.01 vs control. (E) Immunocytological double-staining for collagen type I (red) and α-actinin (green). (F) Quantification of cell surface tracing, *:p<0.05.*

Cellular characterization of fibrotic myocardial cultures

At day 9 of culture, fibrotic cultures contained 61.5±2.6% MFBs whereas control cultures, treated with the antiproliferative agent mitomycin-C, contained 18.9±2.4% MFBs (P<0.001) (Supplemental figure 2A and B). Immunocytological staining revealed intercellular Cx43 expression at MFB-MFB, CMC-CMC and CMC-MFB junctions (Supplemental figure 2C). Heterocellular coupling was confirmed by calcein dye transfer between CMCs and MFBs (data not shown). Expression levels of Cx43 at heterocellular CMC-MFB junctions were significantly lower than at homocellular CMC-CMC junctions (35.5±12.3 vs. 7.8±3.1 arbitrary

units, *P*<0.0001) (Supplemental figure 2D). Importantly, as fibrotic cultures did not show an increase in cell surface area (1.2±0.46 10^6 pixels in control cultures vs. 1.1±0.35 10^6 pixels in fibrotic cultures) or up regulation of ANP expression (16.8±4.8 vs. 17.3±6.6 arbitrary units in control and fibrotic cultures, respectively, p=ns), absence of a hypertrophic component was confirmed (Supplemental figure 2E and 2F).

Conduction and repolarization are slowed in fibrotic and in hypertrophic cultures

Optical mapping recordings similarly showed slow conduction in uniformly propagating hypertrophic and fibrotic cultures (12.2±2.5 and 13.2±3.0 cm/s, respectively, vs. 24.5±2.1 cm/s in controls, *P*<0.0001) (Figure 1A). APD_{80} restitution curves from spontaneous optical signals showed prolonged repolarization compared to control cultures, which was most pronounced at activation frequencies ≤1 Hz (238±65 ms in control [range of 157-393 ms] vs. 721±404 ms [range of 396-1842] and 820±681 ms [range of 400-2474 ms], *P*<0.001 and *P*<0.05 respectively) (Supplemental Figure 3 and Figure 1B). Apart from AP prolongation, AP triangulation (APD_{30}-APD_{90}) was significantly increased (140±59 ms in control vs. 303±117 ms and 298±64 ms in hypertrophy and fibrosis, *P*<0.05) (Figure 1C, 1D and 1E). Furthermore, the maximal spatial APD_{80} dispersion was higher in both pathological substrates (240±92ms in hypertrophic and 233±151ms in fibrotic cultures vs. 53±36ms in controls, *P*<0.01) (Figure 1F), suggesting increased heterogeneity of repolarization in hypertrophic or fibrotic cultures.

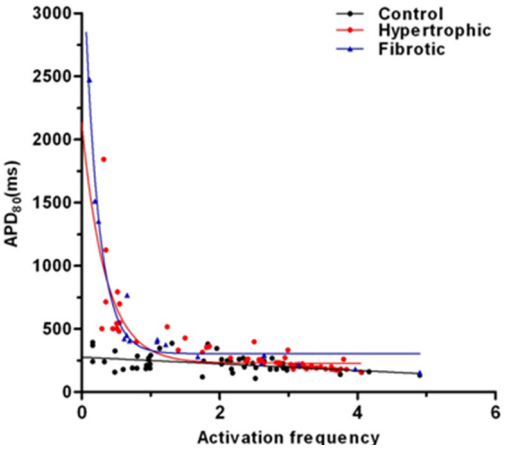

Supplemental Figure 3: *APD_{80} restitution curve shows that the slope of APD_{80} restitution strongly increases at activation frequencies below 1 Hz in hypertrophic or fibrotic cultures.*

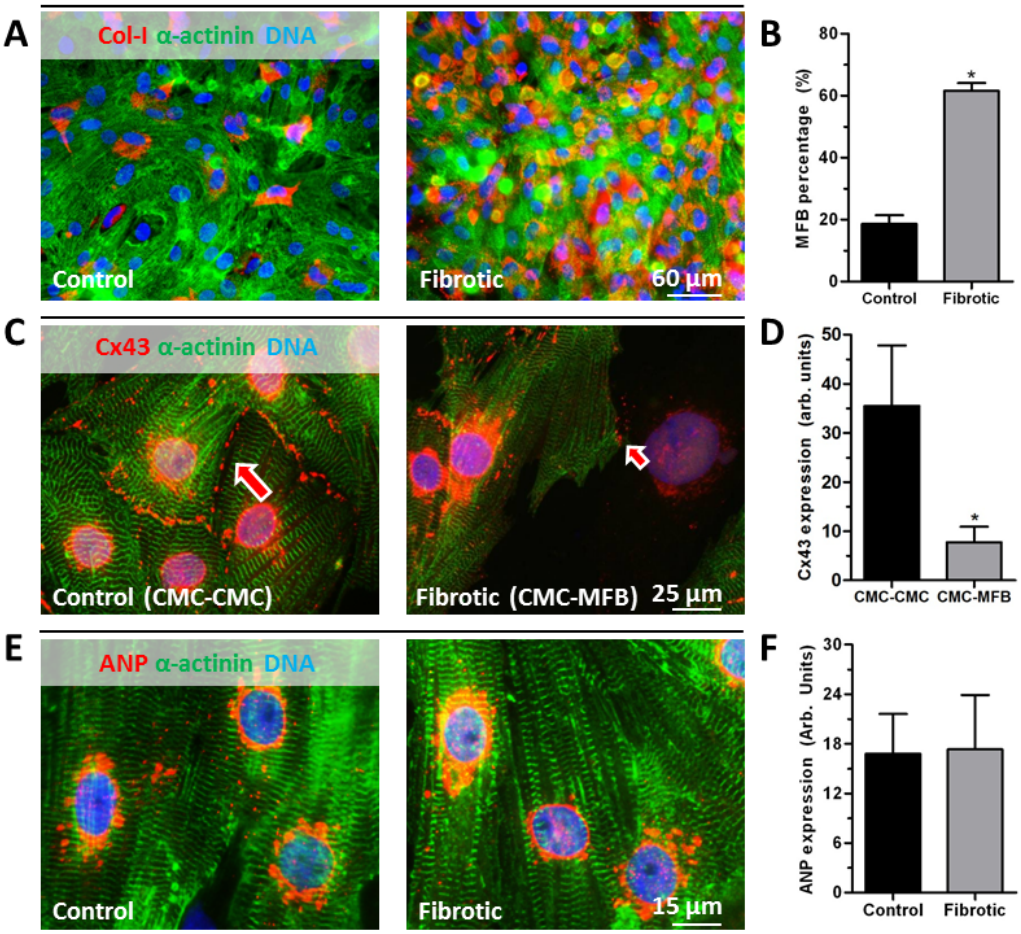

Supplemental Figure 2. *Cellular characterization of fibrotic myocardial cultures. (A) Typical examples of immunocytological double-staining for collagen-I (red) and α-actinin (green) (B) Quantification of MFB count by collagen-I signal *:p<0.0001 vs control (C) Immunocytological double-staining of Cx43 (red) and α-actinin (green) showing homocellular (red arrow) and heterocellular Cx43 expression (indicated by small red arrow) between CMCs (green) and MFBs. (D) Quantification of homocellular (CMC-CMC) and heterocellular (CMC-MFB) Cx43 expression. *:p<0.001 vs control. (E) Typical examples of ANP (red) and α-actinin (green) double-staining. (F) Quantification of ANP signal.*

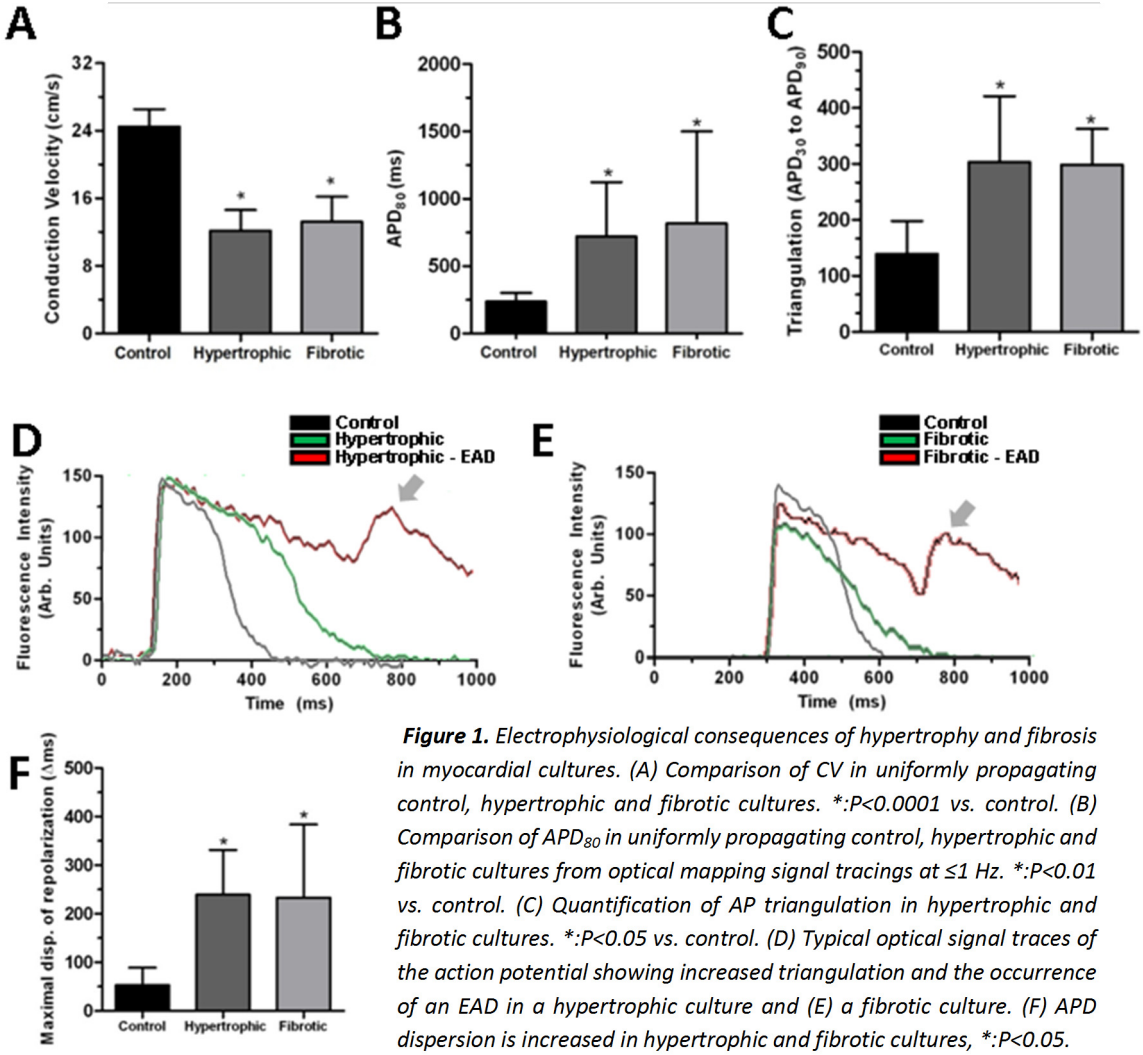

Figure 1. *Electrophysiological consequences of hypertrophy and fibrosis in myocardial cultures. (A) Comparison of CV in uniformly propagating control, hypertrophic and fibrotic cultures. *:P<0.0001 vs. control. (B) Comparison of APD_{80} in uniformly propagating control, hypertrophic and fibrotic cultures from optical mapping signal tracings at ≤1 Hz. *:P<0.01 vs. control. (C) Quantification of AP triangulation in hypertrophic and fibrotic cultures. *:P<0.05 vs. control. (D) Typical optical signal traces of the action potential showing increased triangulation and the occurrence of an EAD in a hypertrophic culture and (E) a fibrotic culture. (F) APD dispersion is increased in hypertrophic and fibrotic cultures, *:P<0.05.*

Triggered activity caused by abnormal repolarization gradients underlies focal tachyarrhythmias that occur in fibrotic and hypertrophic cultures

Apart from prolonged repolarization in fibrotic or hypertrophic cultures, triggered activity due to EADs was frequently observed. The incidence of EADs in both hypertrophy (40%, n=25) and fibrosis (65.5%, n=29) was significantly higher compared to control cultures (4.2%, n=24) (Figure 2D). The occurrence of EADs not only lengthened APD_{80}, but also dramatically increased the spatial heterogeneity of repolarization (from 197±78ms during uniform repolarization to 1570±1155ms during EADs, *P*<0.05, Supplemental Figure 4). EADs could be observed spontaneously but were also easily evoked by 1Hz stimulation in both substrates. Additionally, EADs could repeatedly oscillate.

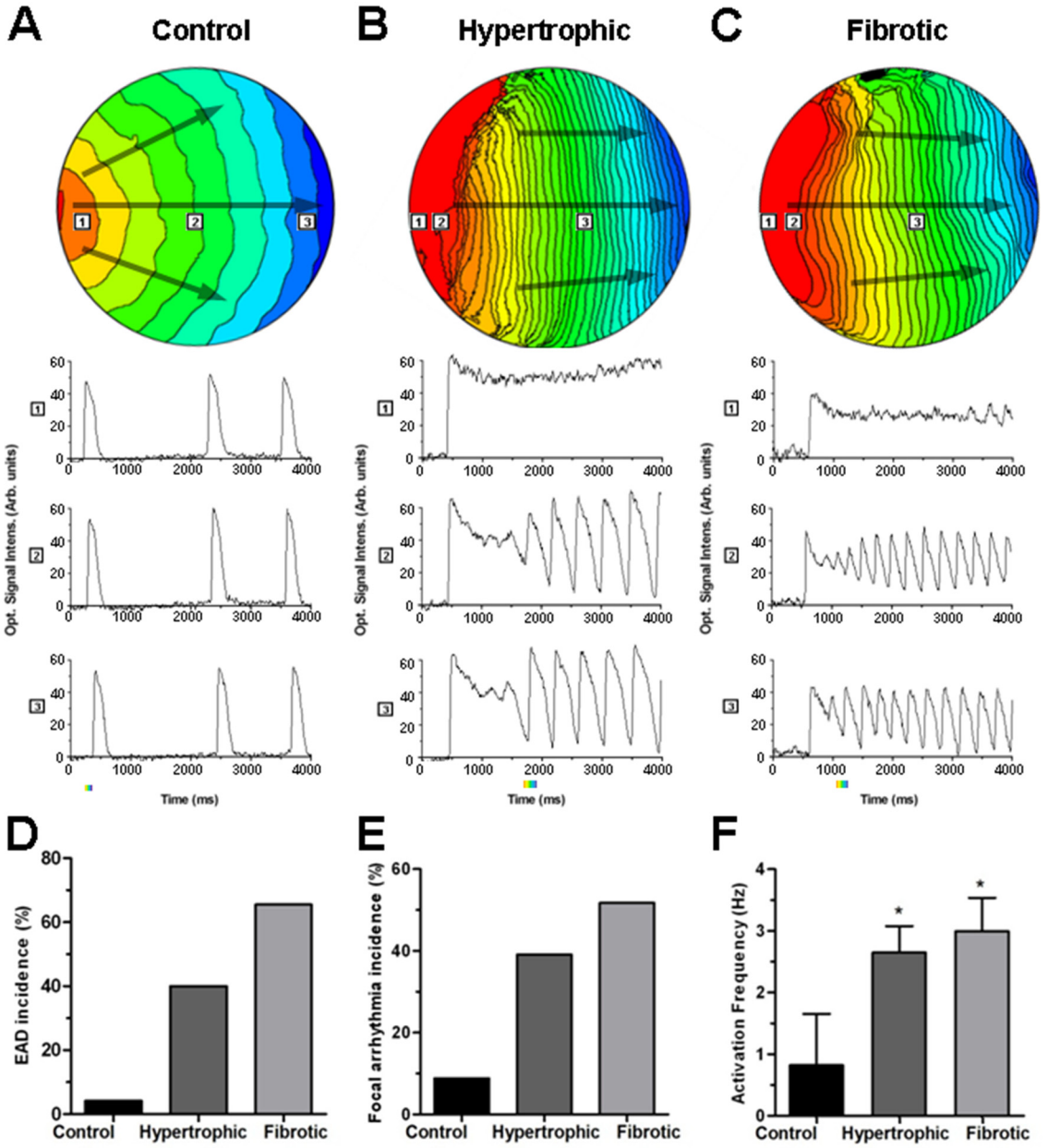

Figure 2. *Spontaneous focal tachyarrhythmias are formed in both hypertrophic and fibrotic myocardial cultures by repetitive EADs. (A) Typical example of an activation map of an uniformly propagating control culture (6 ms isochronal spacing). Corresponding non-high-pass filtered and spatially filtered optical signals indicated by numbers 1-3 show short APDs and low activation frequency. Black arrows indicate the diverging direction of AP propagation as a result of the convex waveform. (B) Activation map of focal tachy-arrhythmic activation in a hypertrophic or (C) fibrotic culture (6ms isochrones spacing). Corresponding optical signals show ceased repolarization at point 1, initiation of the first EAD*

*after slow repolarization in point 2 followed by several propagated EADs and propagation of the first and following EADs in point 3 resulting in a high activation frequency. Black arrows indicate converging/planar direction of AP propagation. (D) Incidence of EADs and (E) spontaneous focal arrhythmias. (F) Repetitive focal activation increases activation frequency in both substrates when compared with normal, uniformly propagating control cultures. *:P<0.001 vs. control.*

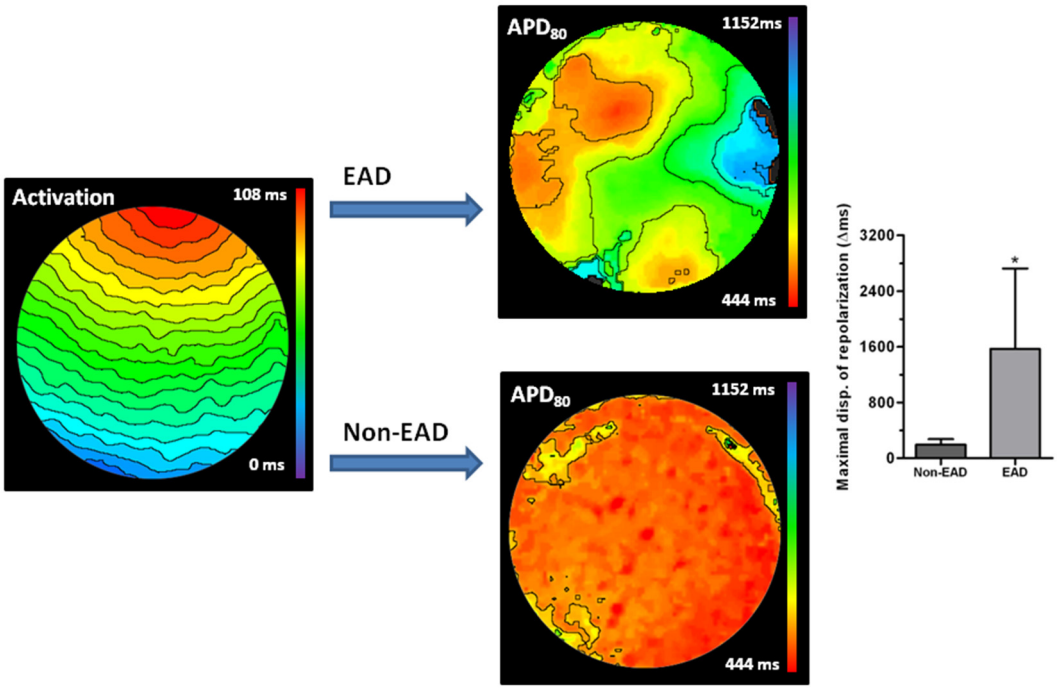

Supplemental Figure 4: *Effect of EADs on APD dispersion. Examples are taken from fibrotic cultures but are also representative for hypertrophic cultures. Uniform activation is shown on the left (6 ms isochrones). After such activation, repolarization occurs throughout the culture (bottom-right repolarization map). However, repolarization can reverse in fibrotic or hypertrophic cultures. The resulting EADs greatly lengthen local APDs (top-right repolarization map), which considerably enhances spatial APD dispersion. This creates a substrate that is vulnerable to reentrant conduction as enhanced differences in refractoriness facilitate formation of unidirectional block. The same observations were made in hypertrophic cultures.*

Triggered activity resulted in an increased activation frequency (2.64±0.42 Hz in hypertrophic or 2.99±0.54 Hz for fibrotic cultures vs. 0.82±0.83 Hz in uniformly conducting control cultures, both *P*<0.001 vs. control) (Figure 2F), thereby identifying this activation pattern as a focal tachyarrhythmia. These focal arrhythmias were infrequently observed in controls (8.8%, n=57, Figure 2A), but were prominent in both hypertrophic (39.1%, n=23) (Figure 2B) and fibrotic cultures (51.7%, n=29, Figure 2C, 2E). During focal tachyarrhythmias, repolarization locally ceased, (Figure 2B and C, point 1) resulting in a sustained depolarized

area in both substrates. As a consequence of juxtaposed repolarizing tissue and the resulting repolarization gradient, tissue at the border of the sustained depolarized area (Figure 2B, C point 2) repolarized very slowly. This translated to a diminished maximal repolarizing down stroke velocity in these areas (0.71±0.16 in controls vs. 0.26±0.04 in hypertrophic and 0.251±0.06 arbitrary optical units/ms in fibrotic cultures, $P<0.001$), thereby providing a prolonged time window for reactivation of the depolarizing force, which could lead to EAD formation. As the membrane potential of tissue distal from the constitutively depolarized area lowers again after the triggered action potential, repolarization in proximity of the depolarized area again occurs slowly. This provided an opportunity for subsequent EADs, persistently repeating the previous sequence of events.

Both hypertrophy and fibrosis cause spontaneous reentrant tachyarrhythmias by critically timed EADs

Interestingly, both hypertrophic (n=111) and fibrotic cultures (n=107) showed a high incidence of spontaneous reentrant tachyarrhythmias, whereas control cultures (n=102) exhibited uniform and fast propagation (Figure 3A, 3B and 3C). Spontaneous reentry incidence was 67.5%, 78.5% and 2.9% in hypertrophic, fibrotic and control cultures, respectively (Figure 3D). To investigate the mechanisms behind these high incidences, reentry formation was studied in these cultures. Spontaneous reentry formation in both substrates was found to be a consequence of triggered activity caused by EADs. The common determinant of reentry initiation was the critical timing of EADs, which is described hereafter. During EADs, APD was increased in both hypertrophic and fibrotic cultures compared to controls (Figure 3B and C, point 1) prior to reentrant conduction, as was the case for APD dispersion (Supplemental Figure 4). Consequentially, hypertrophic and fibrotic cultures were vulnerable to conduction block following EADs. These EADs typically formed at the edge of an area with long APD (Figure 3B and C, point 2) where down stroke velocity of repolarization was locally slowed and thus could prolong the time frame for reactivation of depolarizing current (Figure 3B and C, point 2). If an EAD was generated, this newly generated EAD propagates away from the area with the long APD, as the AP will only meet relatively well-repolarized tissue in that direction (Figure 3B and C point 3). Thereby, unidirectional conduction block was formed (Figure 3, indicated by double black lines). If repolarization occurred at the site of EAD origin before return of the wave front, reentry was enabled by such critical timing. This resulted in increased activation frequency (0.82±0.83Hz in uniformly conducting controls vs. 3.22±0.41Hz in hypertrophic or 3.93±0.66Hz in fibrotic cultures showing reentry $P<0.0001$) (Figure 3E, 3F and 3G) identifying this conduction pattern as another type of tachyarrhythmia.

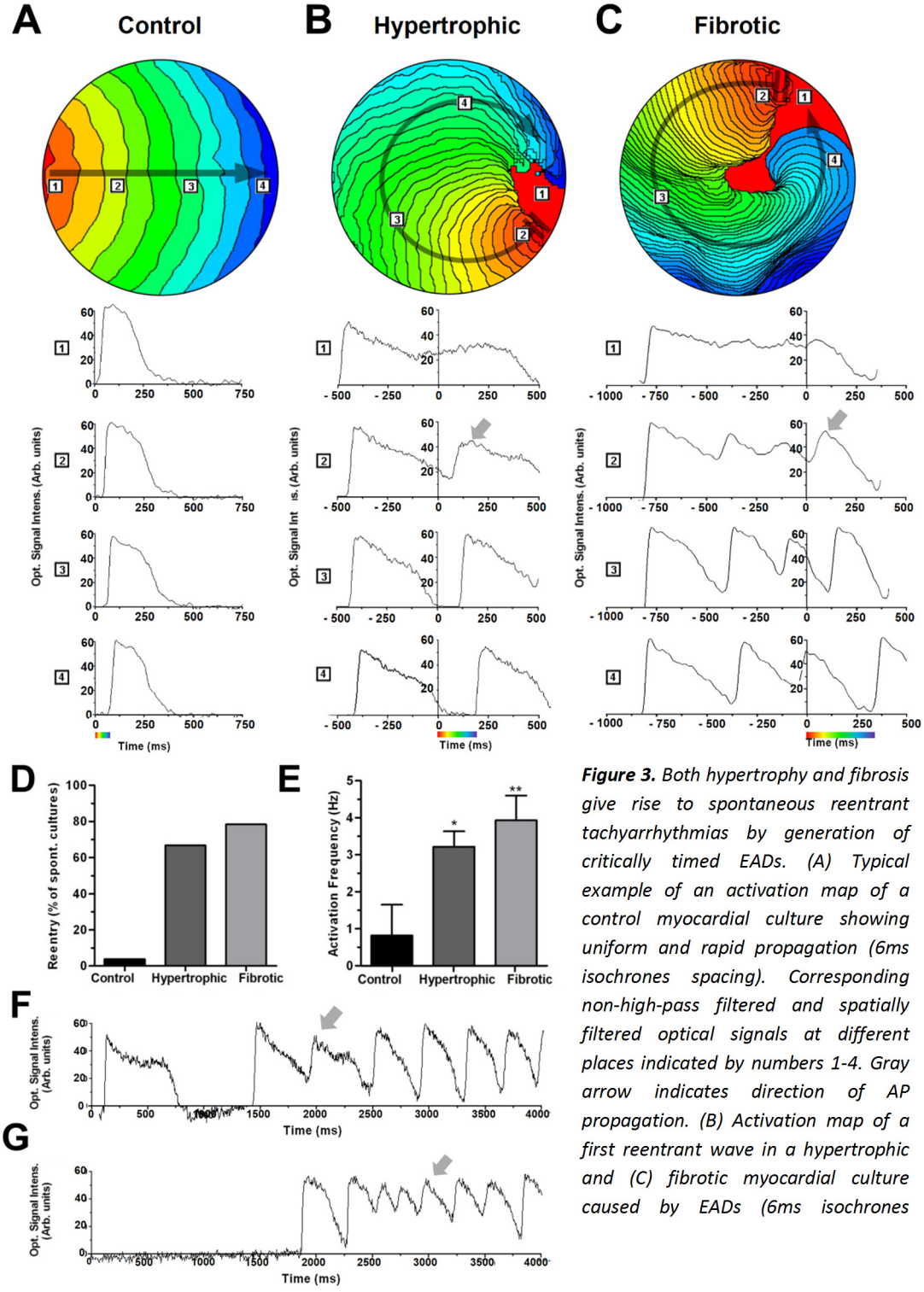

Figure 3. *Both hypertrophy and fibrosis give rise to spontaneous reentrant tachyarrhythmias by generation of critically timed EADs. (A) Typical example of an activation map of a control myocardial culture showing uniform and rapid propagation (6ms isochrones spacing). Corresponding non-high-pass filtered and spatially filtered optical signals at different places indicated by numbers 1-4. Gray arrow indicates direction of AP propagation. (B) Activation map of a first reentrant wave in a hypertrophic and (C) fibrotic myocardial culture caused by EADs (6ms isochrones*

*spacing). Corresponding optical signals at places indicated by numbers 1-4. Gray arrow indicates the critically timed EAD. Double black lines indicate unidirectional block, black arrow indicates direction of AP propagation. (D) Incidence of spontaneous reentrant tachyarrhythmias. (E) Activation frequency in normal, uniformly propagating control cultures compared to hypertrophic or fibrotic cultures showing reentrant conduction. *:P<0.0001 vs. control, **:P<0.0001 vs. control and hypertrophic cultures. (F) Typical example of a full AP trace of a hypertrophic and (G) fibrotic culture, showing a critically timed EAD (gray arrow) followed by a reentrant tachyarrhythmia.*

Substrate-specific effects on electrophysiological properties of CMCs

To investigate substrate-specific effects on CMCs, protein expression of several ion channels and Cx43, as well as action potentials were investigated in all groups. Expression of Kv4.3 was decreased by 29%, in hypertrophic CMCs compared to controls (p=0.015). Expression of Nav1.5, Cav1.2, Kir2.1, and Kv7.1 were not significantly altered in hypertrophic cultures (Figure 4A,B). In contrast to hypertrophic cultures, CMCs in fibrotic cultures exhibited significantly higher expression of Kir2.1 only, compared to CMCs in control cultures (p=0.048 vs. control, Figure 4A, C). However, this difference is most likely not attributable to electrical remodeling, but to Kir2.1 expression in myofibroblasts contributing to the overall Kir2.1 expression when corrected for α-actinin.[10] Expression of intercellular Cx43 between CMCs at the protein level was decreased in hypertrophic cultures, while in fibrotic cultures, intercellular protein expression of Cx43 between CMCs was unaltered (12.2±7.1 arbitrary units in hypertrophy vs. 32.8±10.9 and 33.5±10.2 in control and fibrosis, *P*<0.01) (Figure 4D and 4E). Intracellular membrane potential recordings revealed distinctly different action potential morphologies (Figure 4E); with wide action potentials in hypertrophic CMCs and CMCs in fibrotic cultures and narrow action potentials in control CMCs. Furthermore, CMCs in fibrotic cultures were depolarized as maximal diastolic potentials were -48±7 mV (n=12, *P*<0.0001 vs. control) whereas hypertrophic CMCs showed no such alteration (-62±6 mV, n=8, p=ns) compared with control (-66±7 mV, n=8) (Figure 4F and 4G). Importantly, maximal diastolic potential of CMCs in fibrotic cultures became more negative after gap-junctional uncoupling with 25 µM 2-APB (-59±4 mV (n=5) vs. -48±7 mV (n=12) in untreated fibrotic cultures respectively. In contrast, CMCs in hypertrophic or control cultures showed no significant change after 2-APB in maximal diastolic potential (-62±6 mV without vs. -65±4 mV with 2-APB in hypertrophic cultures, p>0.05 n=4 and -66±7 without vs. -68±5 mV with 2-APB in control cultures, p>0.05, n=4). Moreover, APD_{80} was strongly reduced in CMCs in fibrotic cultures after uncoupling (608±20ms without vs. 286±32ms with 2-APB, *P*<0.05, n=5) while APD_{80} remained largely unchanged after uncoupling CMCs in hypertrophic (732±26ms without vs. 715±23ms with 2-APB, p>0.05, n=4) or CMCs in control cultures (216±11ms without vs. 202±13ms with 2-APB, p>0.05). These data imply intrinsic electrical remodeling that decreases repolarization reserve as a pro-arrhythmic mechanism of

hypertrophy, as opposed to extrinsic MFB-induced depolarization as a pro-arrhythmic mechanism of fibrosis.

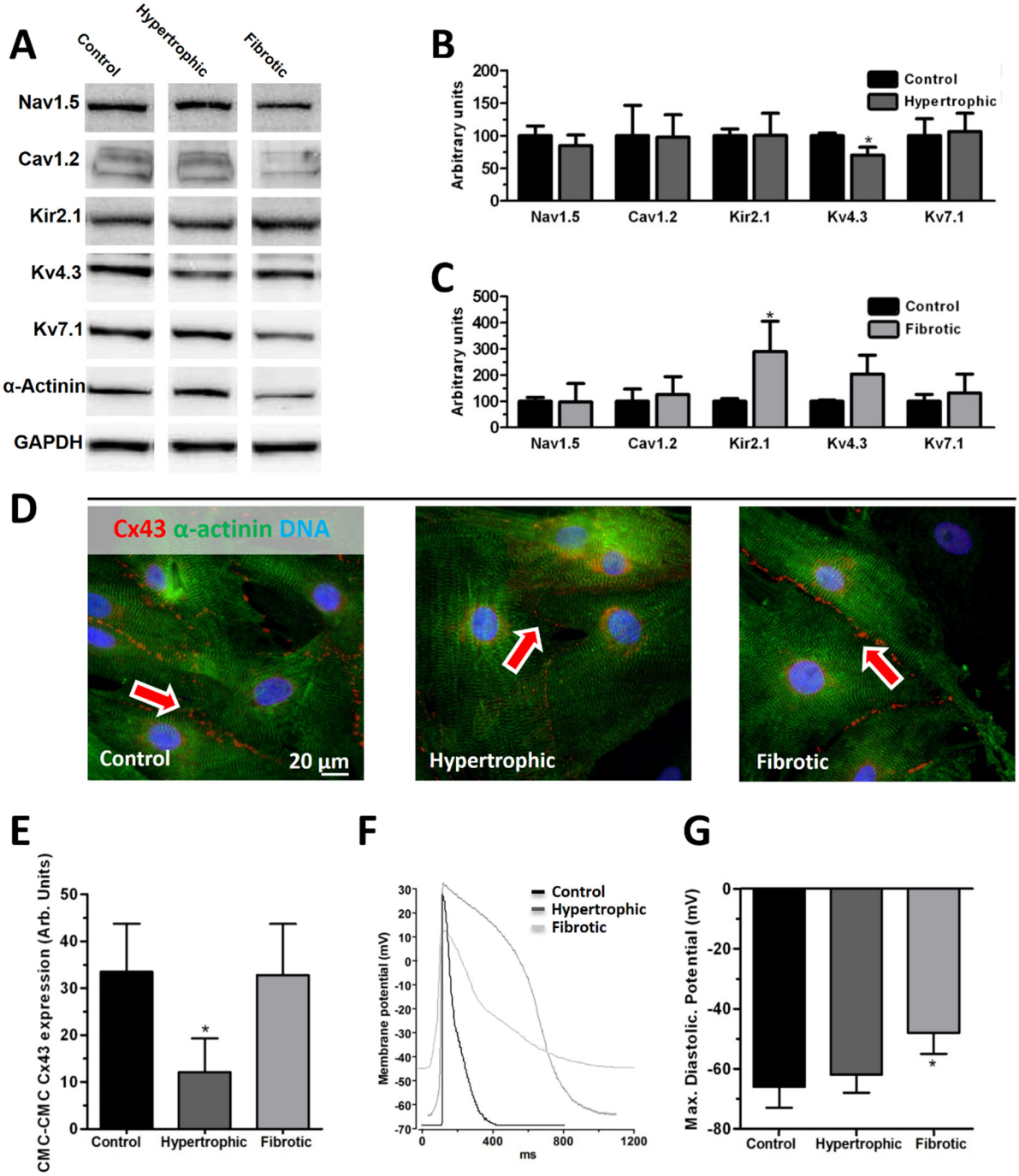

Figure 4. *Conduction slowing and AP triangulation are associated with either ion channel- and gap junctional remodeling or MFB-induced depolarization. (A) Typical examples of protein expression profiles in hypertrophic, fibrotic or control cultures as visualized by Western Blot analysis. (B) Quantification of ion channel protein expression corrected for corresponding GAPDH expression and α-actinin in control and hypertrophic cultures (*:P<0.01) and (C) control and fibrotic cultures. (D) Immunocytological staining of α-actinin (green) and Cx43 (red) in control, hypertrophic or fibrotic cultures. (E) Quantification of intercellular Cx43 signal, *:P<0.01. (F) Current-clamp traces of action potential in control, hypertrophic and fibrotic cultures. (G) Quantification of maximal diastolic potential. *:P<0.001.*

Substrate-specific effects of pharmacological interventions imply differing pro-arrhythmic mechanisms

To further characterize differences between pro-arrhythmic mechanisms of hypertrophy and fibrosis, *in vitro* effects of several drugs on arrhythmogeneity were compared between hypertrophic and fibrotic myocardial cultures. Single point 1Hz stimulation for 10 ms evoked focal or reentrant arrhythmias in hypertrophic and fibrotic cultures (Figure 5A, lower records) with incidences of 75% in hypertrophy, 78% in fibrosis and 3% in control. To study the role of reduced repolarization reserve in arrhythmogeneity, 0.5 mmol/L sotalol was administered to control cultures, prolonging APD_{80} to 118% of initial values. Moreover, cultures showed EADs and reentrant arrhythmias after sotalol, which thereby increased arrhythmic incidence from 0% to 50% (n=16). L-type calcium channels were blocked by 3 µM nitrendipine, which is expected to lower net inward current and thereby reduce APD and arrhythmia incidence. In both hypertrophic and fibrotic cultures, no EADs, focal or reentrant arrhythmias could be evoked after nitrendipine (n=25 and n=15 for hypertrophic and fibrotic cultures) (Figure 5B and 5C). Pacing at 1Hz after nitrendipine administration resulted in electrical capture in all hypertrophic cultures (n=24), and shortening of APD_{80} (57.7±7.2% of untreated cultures, P<0.001) (Figure 5B), while 9 out of 19 fibrotic cultures were rendered unexcitable (Figure 5B and 5C). In line with these results, 10 µM verapamil treatment fully prevented formation of arrhythmias in both groups, but produced conduction block in fibrotic cultures (11 unexcitable cultures out of 15) (Figure 5B and 5C), while all hypertrophic cultures remained excitable (n=14). To investigate the effect of blockade of the fast sodium channel in the different substrates, 20 µM TTX was administered to hypertrophic or fibrotic cultures in another set of experiments. Before TTX administration, arrhythmic incidence was 13 out of 22 hypertrophic cultures and 12 out of 19 fibrotic cultures. In 16 controls, no arrhythmias were detected. Following TTX administration, EAD incidence remained largely unchanged, as incidences were 16 out of 22 hypertrophic cultures and 11 out of 19 fibrotic cultures, making nav1.5-dependent mechanisms of EADs unlikely in the tested cultures. To test the contribution of altered intracellular calcium handling to arrhythmogenesis in these models, all intracellular calcium was buffered by treatment with 10-50 µM BAPTA-AM in an optical mapping experiment.

Interestingly, BAPTA-AM treatment did not decrease arrhythmia incidence in hypertrophic nor fibrotic cultures (90%, n=40 and 76%, n=39, respectively) compared to non-treated cultures. These findings demonstrate that generation of EADs in these substrates is largely independent of intracellular calcium handling.

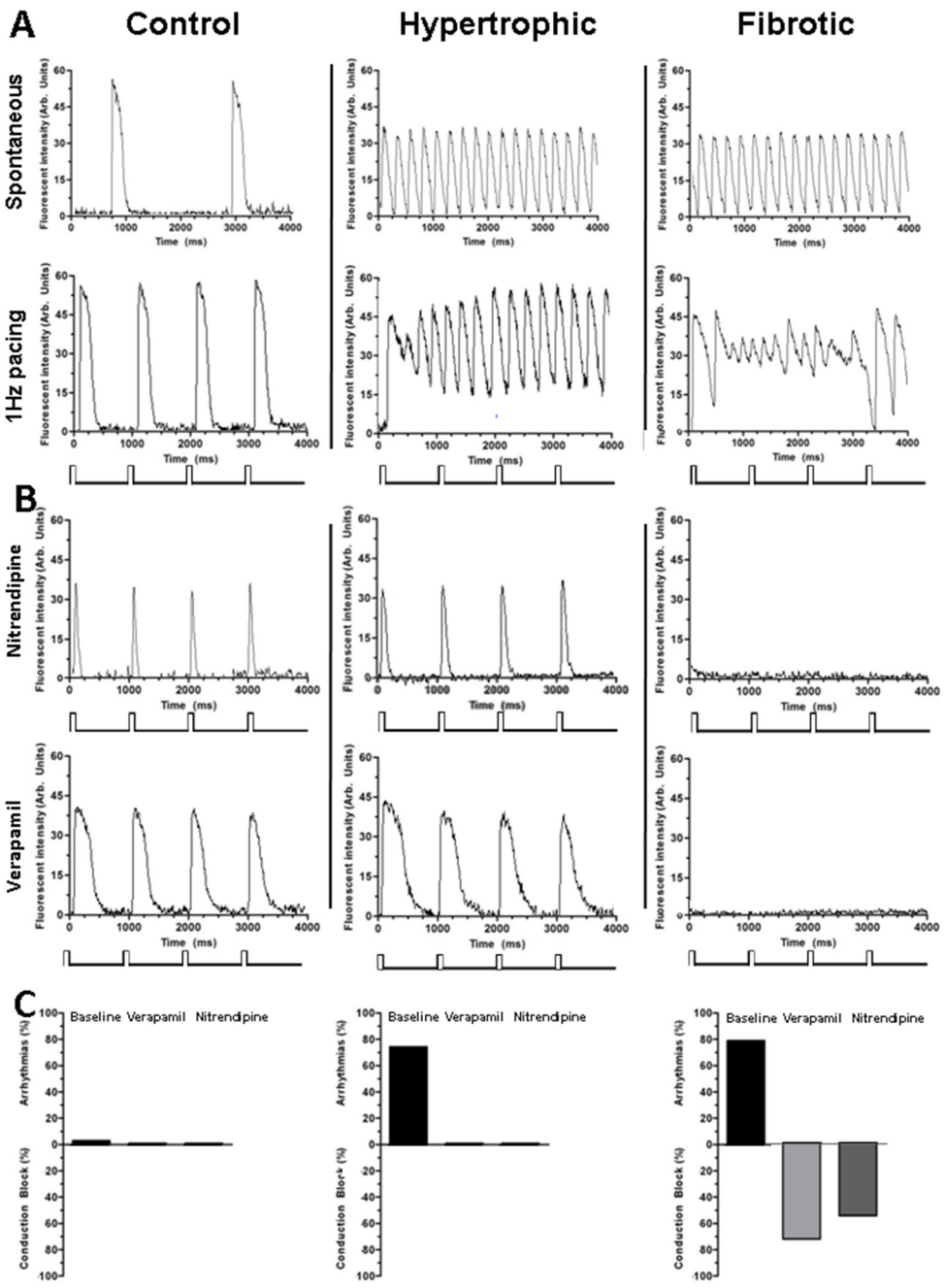

Figure 5. *Substrate-specific effects of L-type calcium channels blockade on arrhythmogeneity. (A) Typical examples of spatially and non-high-pass filtered optical signal traces, occurring spontaneously (above) and during 1Hz pacing (below) in untreated control (left), hypertrophic (middle) and fibrotic (right) cultures. (B) Same traces during 1Hz pacing in control (left), hypertrophic (middle) and fibrotic (right) cultures after treatment with 3 μM nitrendipine (above) and 10 μM verapamil (below). (C) Quantification of the incidence of spontaneous (focal and reentrant) arrhythmias and conduction block in control (left), hypertrophic (middle) and fibrotic (right) cultures after treatment with 10 μM verapamil or 3 μM nitrendipine.*

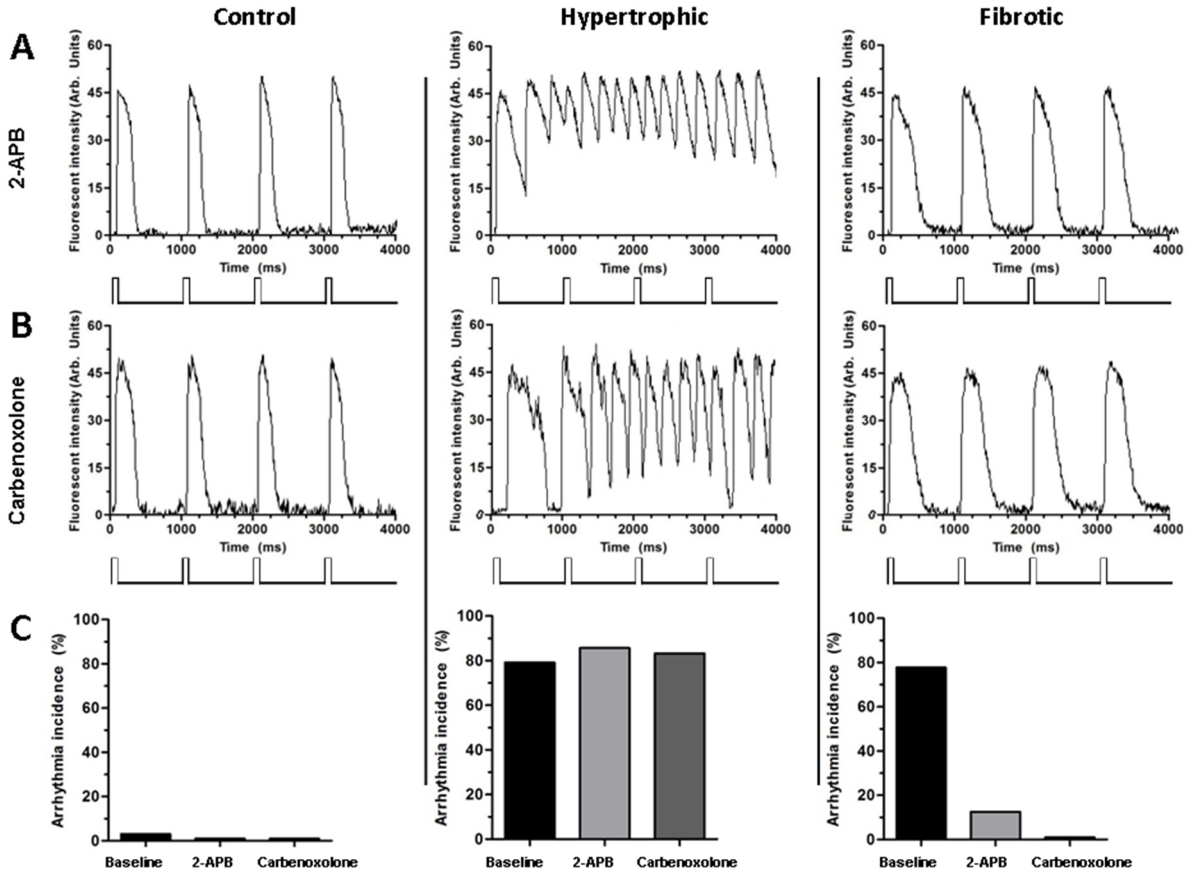

Figure 6. *Effect of gap junctional uncoupling on arrhythmogeneity depends on the arrhythmogenic substrate. (A) Typical examples of spatially filtered and non-high-pass filtered action potential traces during 1Hz pacing in control (left), hypertrophic (middle) and fibrotic (right) cultures after treatment with 5 μM 2-APB or (B) 100 μM carbenoxolone. (C) Quantification of the incidence of spontaneous (focal and reentrant) arrhythmias in control (left), hypertrophic (middle) and fibrotic (right) cultures after treatment with 5 μM 2-APB or 100 μM carbenoxolone.*

As heterocellular coupling is a pro-arrhythmic feature of fibrosis *in vitro*,[11] partial gap junctional uncoupling was performed to further examine differences in arrhythmogeneity of hypertrophic and fibrotic cultures. As MFB-CMC intercellular Cx43 expression is significantly lower than at CMC-CMC junctions (Supplemental Figure 2D), partial uncoupling can lead to inhibition of heterocellular MFB-CMC coupling while preserving sufficient CMC-CMC coupling for propagation. Therefore, cultures were treated with 5 µM 2-APB or 100 µM carbenoxolone. Treatment with 2-APB reduced arrhythmias in fibrotic cultures (12.5%, n=16 vs. 78%, n=18 in untreated fibrotic cultures, $P<0.05$) (Figure 6A and 6C), and decreased APD_{80} (68.7±31.7% of untreated cultures, $P<0.05$). Such anti-arrhythmic effect was absent in hypertrophic cultures (86% arrhythmias n=14, vs. 75% n=12 in untreated hypertrophic cultures) (Figure 6A and 6C). Carbenoxolone also ameliorated arrhythmogeneity in fibrotic cultures, while arrhythmia incidence remained high in hypertrophic cultures (83% arrhythmias, n=12) (Figure 6B and 6C).

Discussion

Key findings of this study are (1) both hypertrophic and fibrotic myocardial cultures give rise to triggered activity causing both focal and reentrant tachyarrhythmias. (2) Underlying pro-arrhythmic mechanisms highly differ between these two pathological conditions; mainly being electrical remodeling of CMCs in hypertrophic cultures or MFB-induced depolarization of CMCs in fibrotic cultures.

Triggered activity, focal and reentrant tachyarrhythmias in experimental models

Cardiac fibrosis and cardiac hypertrophy are both associated with spontaneous tachyarrhythmias.[1-3,12] Traditionally, whole-heart mapping studies suggest either focal or reentrant mechanisms underlying these ventricular tachyarrhythmias.[13,14] However, the complexity of 3-dimensional myocardial tissue hampers complete interpretation of findings and therefore, arrhythmogenesis has also been investigated in experimental 2D and computational models to unequivocally establish the existence of reentrant and focal mechanisms.[15,16] Additionally, despite the spontaneous occurrence of arrhythmias in patients, arrhythmogenesis has been mostly studied by externally applied burst stimulation to force induction of arrhythmias, [17-19] thereby precluding investigation of internal arrhythmic triggers in arrhythmogenesis.

In this study, triggered activity in the form of EADs was found spontaneously and could be evoked by low-frequency stimulation. Moreover, this activity was found to be responsible for the initiation of both focal and reentrant tachyarrhythmias in hypertrophic and fibrotic cultures. It was shown that the onset of focal and reentrant tachyarrhythmias depends on the generation of EADs, which either oscillate during phase 2 or 3 of the AP (focal) or are critically timed to form unidirectional block, slow conduction and thereby facilitate reentry.

The importance of EADs in the onset of ventricular tachycardias is in line with previous *in silico*, *in vitro* and *in vivo* studies.[20,21] Traditionally, this correlation of EADs with arrhythmias was studied by inducing EADs by pharmacological or genetic interventions or, in the case of *in silico* studies, by altering ion channel properties to reduce repolarization reserve. While these studies proved useful to implicate EADs as a principal underlying mechanism of arrhythmogeneity**,** it remained unclear how prevalent acquired cardiac diseases such as hypertrophy or fibrosis may lead to arrhythmias. For hypertrophy, spontaneous EAD generation has been demonstrated in isolated CMCs.[22,23] The current study shows that EADs in hypertrophy also overcome electrotonic load and propagate in 2-dimensional tissue. Additionally, how predicted source-sink mismatching of propagated EADs is overcome is illustrated by the concave waveform (Figure 2B, C) found during focal tachyarrhythmias. This is in accordance with calculations that show that EAD propagation is favored in concave activation as such waveform morphology helps to overcome the source-sink mismatch that determines the threshold of EAD propagation.[24]

As EADs are reactivations of depolarizing current during repolarization, slowed repolarization is a critical facilitating factor for EAD generation. This was demonstrated in the present study by adding sotalol to control cultures, which prolonged APD and caused focal tachyarrhythmias. In addition, dispersion of repolarization causes steep repolarization gradients, which may provide the depolarizing force necessary for reactivation.[25] This reactivation was mainly calcium-dependent, as Nav1.5 blockade had no pronounced anti-arrhythmic effect in either hypertrophic or fibrotic cultures. Additionally, intracellular calcium buffering was ineffective to prevent EADs and arrhythmias while Cav1.2 blockade ameliorated EADs. Findings of prolonged and dispersed repolarization may readily explain the similar pro-arrhythmogenic findings of triggered activity in hypertrophic or fibrotic tissue. However, the similarities between pro-arrhythmogeneity of hypertrophy and fibrosis end at the cellular level of the mechanisms of repolarization prolongation and dispersion.

Substrate-specific pro-arrhythmic mechanisms in cardiac hypertrophy and fibrosis

During cardiac remodeling, hypertrophy and fibrosis may develop to varying degrees. As a result, the resulting pro-arrhythmic features found in cardiac remodeling remain incompletely understood, as concomitance of these substrates precludes distinction between pro-arrhythmic mechanisms of these substrates and therefore, hamper the development of novel anti-arrhythmic treatment modalities. In this study, cellular and ionic mechanisms of arrhythmogeneity substantially differed between cardiac fibrosis and hypertrophy. In fibrosis, fibroblast proliferation and extracellular matrix deposition are known to extrinsically alter cardiac action potential propagation by forming spatial separations between CMCs, which reduces cell-to-cell contact, favors zigzag conduction and provides anatomic obstacles that increase the propensity towards arrhythmias.[26,27] [17].

However, in recent years, focus has shifted towards the MFB in cardiac fibrosis as a possible key factor in the extrinsic pro-arrhythmic mechanisms of fibrosis.[28-31] In culture, MFBs can inactivate voltage-gated potassium channels by depolarizing CMCs and thereby preclude proper repolarization and facilitate EAD generation.[11,12,32] This study confirms these extrinsic effects on CMCs, as high MFB content in cardiac cultures was associated with depolarized membrane potentials in CMCs, prolonged APD_{80} and an increased incidence of EADs that ultimately led to tachyarrhythmias. Other studies showed that paracrine factors secreted from cardiac fibroblasts were also able to induce a certain degree of ion channel remodeling in CMCs, although no EADs were reported in these CMCs.[33] However, no such effects were detected if cardiac fibroblasts were directly co-cultured with CMCs, as was done in the present study. In our study fibrosis led to an increase in Kir2.1 expression when corrected for alpha actinin. However, this is unlikely the result of a functional overexpression of Kir2.1 in cardiomyocytes. In the hypothetical case of functional kir2.1 overexpression in CMCs the MDP in fibrotic cultures would be more negative after uncoupling compared to non-fibrotic controls, while the opposite is true. This means that either the extra kir2.1 is derived from myofibroblasts or does not lead to an increase in inward rectifier current. Furthermore, Findings of strong anti-arrhythmic effects of partial uncoupling confirm dominance of coupling-based pro-arrhythmic mechanisms over paracrine mechanisms in the currently used model. This anti-arrhythmic effect is possibly due to the vast functional reserve capacity of CMC-CMC coupling, which is considerably lower in MFB-CMC coupling and thereby allows for heterocellular uncoupling.[34]

In contrast to fibrosis, partial uncoupling had no anti-arrhythmic effects in hypertrophic tissue indicating differing pro-arrhythmic mechanisms. Reduction of total expression and altered distribution of Cx43 are all features of pathologically hypertrophied myocardium that compromise proper intercellular conduction and thereby lead to conduction slowing.[354] In addition, repolarization reserve is diminished by down regulation of voltage-gated potassium channels, which may increase the propensity towards EADs and ultimately towards arrhythmias.[365] In our study, lowered Cx43 expression, increased ANP and altered ion channel protein expression were confirmed in hypertrophic CMCs, and absent in CMCs in fibrotic and control cultures (Supplemental Figures 1, 2 and Figure 4 C, D). The down regulation of Kv4.3, which contributes to the transient outward current (I_{to}) was in accordance with other studies.[37,387] Hoppe et al showed that a reduction in I_{to} leads to a marked increase in APD by an increase in the plateau potential, thereby altering the early trajectory of repolarization.[398]

Due to differences in pro-arrhythmic mechanisms, L-type calcium channel blockade shortened APD and was anti-arrhythmic in hypertrophic cultures but blocked conduction in fibrotic cultures as propagation in such cultures was largely dependent on calcium channels

due to MFB-induced depolarization and concomitant inactivation of fast sodium channels. Nevertheless, the arrhythmogenic pathways of hypertrophy and fibrosis converge at the point of prolongation of repolarization, APD dispersion and EAD formation. These results suggest that lowering the incidence of spontaneous arrhythmias by preventing EAD generation may require a different approach in hypertrophic or fibrotic-substrates. Alternatively, common pro-arrhythmic factors should be targeted. Future research is needed to elaborate on the implications these findings may have for the *in vivo* setting.

Study Limitations

In our study, fibrosis was mimicked by MFB proliferation in myocardial cultures. However, the deposition of extracellular matrix as another component of fibrosis was not investigated, as *in vitro* deposition of matrix comparable to *in vivo* quality and quantity is difficult to achieve. Although it is well established that MFBs and CMCs functionally couple *in vitro*, strong, undeniable proof of this phenomenon *in vivo* has yet to appear. The implications of changes in expression of Kv4.3 protein found in hypertrophic rat cells cannot be directly extrapolated to human hearts due to differences in expression levels and functions of the associated currents. Consequently, this study establishes an *in vitro* proof-of-principle of cellular pro-arrhythmic mechanisms and recognizes that more *in vivo* research is necessary before this kind of *in vitro* results can be translated to clinical implications.

Conclusions

Hypertrophic and fibrotic myocardial tissues are independent, pro-arrhythmic substrates. Both substrates are characterized by slow conduction, APD prolongation, formation of EADs and subsequent focal and reentrant tachyarrhythmias. However, while pathological hypertrophy is characterized by electrical remodeling of CMCs, fibrosis is mainly characterized by MFB-induced depolarization of CMCs. These differences may stress the importance of a substrate-based approach in the treatment of cardiac arrhythmias.

Acknowledgements

We wish to thank Dr. W.P.M van Meerwijk for helpful discussions, and Huybert J.F. van der Stadt for excellent technical support.

Sources of funding
This work was supported by the Dutch Heart Foundation (2008/B119) and the Netherlands Organisation for Scientific Research (NWO; VENI grant (91611070), D.A.P).

Conflict of Interest
None declared.

Supplemental Material

Materials and Methods

All animal experiments were approved by the Animal Experiments Committee of the Leiden University Medical Center and conform to the Guide for the Care and Use of Laboratory Animals as stated by the US National Institutes of Health.

Experimental protocol

All control cultures were treated with the antiproliferative agent Mitomycin-C (10 µg/ml, Sigma-Aldrich, St. Louis, MO, USA), to prevent proliferation of endogenously present, α-smooth muscle actinin-positive myofibroblasts (MFBs). For this purpose Mitomycin-C dissolved in PBS was diluted in growth medium (Ham's F10 supplemented with 10% fetal bovine serum (FBS, Invitrogen, Carlsbad, CA, USA), 10% horse serum (HS, Invitrogen) and penicillin (100U/ml) and streptomycin (100 µg/ml, P/S; Bio-Whittaker, Carlsbad, CA, USA) and incubated for 2 hours. Subsequently, cultures were rinsed twice in PBS and once in a 1:1 mixture of DMEM/HAMS F10 supplemented with 5% HS and P/S before being kept on this medium throughout the experiment. To induce hypertrophy, Mitomycin-C treated cultures were exposed to 100 µM phenylephrine (PE, Sigma) for 24h at day 3 and day 8[4]. To mimic fibrosis, endogenously present MFBs were allowed to proliferate freely, by treatment with PBS instead of Mitomycin-C. Fibrotic cultures were rinsed identically as control cultures control and hypertrophic cultures after Mitomycin-C/PBS treatment. For reasons of comparability, fibrotic cultures and control cultures received PBS instead of PE.

Immunocytological analyses

Immunocytological stainings were performed as described in earlier studies.[9,40] Cultures were fixed in 1% paraformaldehyde for 20 minutes on ice, after which cultures were rinsed twice with Phosphate Buffered Saline (PBS) and permeabilized with 0.1% Triton X-100. After 2 subsequent wash-steps, cultures were incubated overnight with primary antibodies diluted in PBS with 1% Fetal Bovine Serum. Primary antibodies were directed against α-actinin (Sigma), α-smooth muscle actinin (Sigma), α-skeletal muscle actinin (Abcam, Cambridge, MA, USA), atrial natriuretic peptide (Abcam) or Collagen type I (Abcam) and used at a dilution of 1:200. Double-staining was performed by using primary antibodies that were raised in either mouse or rabbit host species. Corresponding secondary donkey anti-rabbit or donkey anti-mouse Alexa fluor-conjugated antibodies (Invitrogen) were incubated for 2 hours at room temperature at a dilution of 1:400. After rinsing twice, nuclei of these cultures were counterstained for 5 minutes with Hoechst 33321 (Invitrogen). Following 2 wash steps, stained glass coverslips were mounted in Vectashield mounting medium (Vector Laboratories Inc, Burlingame, CA, USA) to minimize photobleaching. Images of cultures were taken and quantified using dedicated software (Image-Pro Plus, version

4.1.0.0, Media Cybernetics, Silver Spring, MD, USA). Quantification of all staining was performed in at least 6 cultures per group with at least 20 photos taken per culture. Quantification of fluorescent signal intensity was performed in at least 15-fold per photo.

To confirm a pathological hypertrophic phenotype in PE-treated CMCs, cultures were characterized at day 9 for protein expression of the hypertrophic markers atrial natriuretic peptide and α-skeletal muscle actin by immunocytological staining. In addition, cell surface area of CMCs was quantified as another measure of hypertrophy. To confirm fibrosis in cardiac cultures, cultures were stained for collagen-I (Abcam) and positive cells were considered to be MFBs and quantified.[9]

Optical mapping

Propagation of action potentials was investigated on a whole-culture scale in hypertrophic, fibrotic or control cultures using voltage-sensitive dye mapping as described earlier.[9] For reasons of standardization and reproducibility, only cultures without structural inhomogeneities as judged by mapping and light microscopy were included for further analyses. Cardiac cultures were plated out in 24-well plates (Corning) at a cell density of $8x10^5$ cells per well. At day 9, cultures were optically mapped. At least 2 hours after the daily refreshing of culture medium, cultures were incubated with culture medium containing 8 µmol/L di-4-ANEPPS for 15±5 minutes at 37º C in a humidified incubator. Subsequently, cultures were refreshed with serum-free, colorless DMEM/HAMS F10 mixed in a 1:1 ratio. Next, electrical propagation patterns were recorded by optical mapping at 37ºC. Mapping experiments typically did not exceed 30 minutes per 24-wells plate. Also, cultures were not exposed to excitation light for longer than 50 s to limit possible phototoxic effects. Excitation light (e_{ex} = 525±25 nm) was delivered by a halogen arc-lamp (MHAB-150W, Moritex Corporation, San Jose, CA, USA) through epi-illumination. Fluorescent emission light passed through a dichroic mirror and a long-pass emission filter (>590 nm) and was focused onto a 100x100 pixels CMOS camera (Ultima-L, SciMedia, Costa Mesa, CA, USA) by a 1.6x converging lens (Leice, Wetzlar, Germany). This resulted in a spatial resolution of 160 µm/pixel and a field of view of 16 by 16 mm. Spontaneous or stimulated electrical activity was recorded for 6-24 seconds at 6ms exposure time per frame. Data analysis was performed with specialized software (Brainvision Analyze 1101, Brainvision Inc, Tokyo, Japan) after pixels signals were averaged with 8 of its nearest neighbors to minimize noise-artifacts. Conduction velocity (CV), maximal optical action potential upstroke (dF/dT_{max}), maximal action potential downstroke velocity (dF/dTmin), action potential duration until 80% repolarization (APD_{80}) were determined at ≤1 Hz at six different locations equally distributed throughout the culture and averaged before inclusion in further analyses. Spatial dispersion of repolarization was defined as the maximal difference in APD_{80} within a culture and was determined at activation frequencies of ≤1 Hz.

Assessment of EADs and focal tachyarrhythmias

As prevalent reentrant conduction precludes assessment of conduction patterns other than reentry, reentry needed to be eliminated to analyze all possible conduction patterns and spontaneous activity in included cultures. To maintain ion channel properties, reentry had to be eliminated in a non-pharmacological manner. For this purpose, we used a custom-made epoxy-coated platinum electrode and performed unipolar stimulation with 6 V for 4 seconds using an electrical stimulus module with corresponding software (Multichannel Systems), which successfully eliminated reentry in >90% of the cultures. After absence of reentry was confirmed by 2s optical mapping, spontaneous activity was detected by mapping of the cultures for 24 seconds following application of the stimulus. This allowed for detection of EADs and spontaneous focal arrhythmias that otherwise would be overruled by reentrant activation. All cultures included in this analysis, regardless of the presence of reentry, underwent equal stimulation for standardization purposes.

Pharmacological anti-arrhythmic interventions

To investigate the antiarrhythmic potential of pharmacological interventions in different substrates, several pharmacological agents were administered to hypertrophic, fibrotic or control cultures under optical mapping conditions. Inhibition of L-type Ca^{2+} inward current was performed by application of a relatively low dose of verapamil (10 μM) (Centrafarm, Etten-Leur, the Netherlands) or nitrendipine (3 μM) (Sigma) directly into the mapping medium. As this instantly abolished all spontaneous activity in all cultures regardless of composition, cultures were stimulated at 2V (1Hz intervals) for 4 seconds to evaluate capture and propagation parameters. For standardization purposes, arrhythmic activity before verapamil and nitrendipine administration was also investigated following 1Hz stimulation.

To reduce heterocellular coupling between CMCs and MFBs in hypertrophic or fibrotic myocardial cultures, a relatively low dose of the 2-APB (5 μM) (Tocris Bioscience, Bristol, United Kingdom) or carbenoxolone (100 μM) (Sigma) was supplied in the mapping medium and incubated for 20 minutes. To investigate effects of Nav1.5 blockade, tetrodotoxin (TTX, 20 μM, Alomone Labs) was pipetted into the medium and incubated for 10s. For investigation of the involvement of intracellular calcium handling in arrhythmogeneity, intracellular calcium was buffered using 10-50 μM BAPTA-AM (Sigma) which incubated for 20 minutes. To investigate the effect of action potential duration (APD) prolongation on arrhythmogeneity, 0.5 mM sotalol (Sigma) was used. For reproducibility and comparability between all pharmacological interventions, all cultures were paced with a 1 Hz supra-threshold stimulation protocol during optical mapping recordings.

Whole-cell patch-clamp

Whole-cell current-clamp measurements were performed in spontaneously active (0.2-1 Hz) hypertrophic, fibrotic or control cultures. For fibrotic cultures, MFBs were labeled with eGFP using the vesicular stomatitis virus G protein-pseudotyped self-inactivating lentivirus vector CMVPRES as described previously.[9] Subsequently, these labeled MFBs were plated out with CMCs in equal quantity and density as fibrotic cultures with freely proliferating MFBs at day 9. To maintain the initially plated ratio, cultures were treated with mitomycin-C. Therefore, CMCs were easily identifiable in these fibrotic cultures. At day 9, after identification of CMCs by fluorescence microscopy, current-clamp experiments were performed in these cells. Whole-cell recordings were performed at 25°C using a L/M-PC patch-clamp amplifier (3kHz filtering) (List-Medical, Darmstadt, Germany). The pipette solution contained (in mmol/L) 10 Na_2ATP, 115 KCl, 1 $MgCl_2$, 5 EGTA, 10 HEPES/KOH (pH 7.4). Tip and seal resistance were 2.0-2.5 MΩ and >1 GΩ, respectively. The bath solution contained (in mmol/L) 137 NaCl, 4 KCl, 1.8 $CaCl_2$, 1 $MgCl_2$, and 10 HEPES (pH 7.4). In a subset of experiments, CMCs were functionally uncoupled by incubation for 20 minutes with 25 µmol/L 2-APB to investigate intrinsic action potential morphology in hypertrophic, fibrotic or control cultures. For data acquisition and analysis, pClamp/Clampex8 software (Axon Instruments, Molecular Devices, Sunnyvale, CA, USA) was used.

Statistical analysis

Statistical analyses were performed using SPSS11.0 for Windows (SPSS Inc., Chicago, IL, USA). Comparison between numerical data of groups was performed using the student-t test or paired t-test where appropriate. Values were expressed as mean±SD. Significance of differences in incidences between groups was determined by the Chi-square statistical test. Differences were considered statistically significant if $p<0.05$.

References

1. Haider AW, Larson MG, Benjamin EJ, Levy D. Increased left ventricular mass and hypertrophy are associated with increased risk for sudden death. *J Am Coll Cardiol*. 1998;32:1454-1459.

2. McLenachan JM. Ventricular arrhythmias in patients with hypertensive left ventricular hypertrophy. 1987.

3. van der Burg AE, Bax JJ, Boersma E, Pauwels EK, van der Wall EE, Schalij MJ. Impact of viability, ischemia, scar tissue, and revascularization on outcome after aborted sudden death. *Circulation*. 2003;108:1954-1959.

4. Kuck KH, Schaumann A, Eckardt L, Willems S, Ventura R, Delacretaz E, Pitschner HF, Kautzner J, Schumacher B, Hansen PS. Catheter ablation of stable ventricular

tachycardia before defibrillator implantation in patients with coronary heart disease (VTACH): a multicentre randomised controlled trial. *Lancet*. 2010;375:31-40.

5. Zeppenfeld K and Stevenson WG. Ablation of ventricular tachycardia in patients with structural heart disease. *Pacing Clin Electrophysiol*. 2008;31:358-374.

6. Borleffs CJ, van EL, Schotman M, Boersma E, Kies P, van der Burg AE, Zeppenfeld K, Bootsma M, van der Wall EE, Bax JJ, Schalij MJ. Recurrence of ventricular arrhythmias in ischaemic secondary prevention implantable cardioverter defibrillator recipients: long-term follow-up of the Leiden out-of-hospital cardiac arrest study (LOHCAT). *Eur Heart J*. 2009;30:1621-1626.

7. Arshad A, Mandava A, Kamath G, Musat D. Sudden cardiac death and the role of medical therapy. *Prog Cardiovasc Dis*. 2008;50:420-438.

8. Pijnappels DA, Schalij MJ, Ramkisoensing AA, van Tuyn J, de Vries AA, van der Laarse A, Ypey DL, Atsma DE. Forced alignment of mesenchymal stem cells undergoing cardiomyogenic differentiation affects functional integration with cardiomyocyte cultures. *Circ Res*. 2008;103:167-176.

9. Askar SF, Ramkisoensing AA, Schalij MJ, Bingen BO, Swildens J, van der Laarse A, Atsma DE, de Vries AA, Ypey DL, Pijnappels DA. Antiproliferative treatment of myofibroblasts prevents arrhythmias in vitro by limiting myofibroblast-induced depolarization. *Cardiovasc Res*. 2011.

10. Walsh KB and Zhang J. Neonatal rat cardiac fibroblasts express three types of voltage-gated K+ channels: regulation of a transient outward current by protein kinase C. *Am J Physiol Heart Circ Physiol*. 2008;294:H1010-H1017.

11. Askar SF, Bingen BO, Swildens J, Ypey DL, van der Laarse A, Atsma DE, Zeppenfeld K, Schalij MJ, de Vries AA, Pijnappels DA. Connexin43 silencing in myofibroblasts prevents arrhythmias in myocardial cultures: Role of maximal diastolic potential. *Cardiovasc Res*. 2011.

12. Kleber AG and Rudy Y. Basic mechanisms of cardiac impulse propagation and associated arrhythmias. *Physiol Rev*. 2004;84:431-488.

13. Pogwizd SM, Hoyt RH, Saffitz JE, Corr PB, Cox JL, Cain ME. Reentrant and focal mechanisms underlying ventricular tachycardia in the human heart. *Circulation*. 1992;86:1872-1887.

14. de Bakker JM, van Capelle FJ, Janse MJ, Wilde AA, Coronel R, Becker AE, Dingemans KP, van Hemel NM, Hauer RN. Reentry as a cause of ventricular tachycardia in

patients with chronic ischemic heart disease: electrophysiologic and anatomic correlation. *Circulation*. 1988;77:589-606.

15. Allessie MA, Bonke FI, Schopman FJ. Circus movement in rabbit atrial muscle as a mechanism of tachycardia. III. The "leading circle" concept: a new model of circus movement in cardiac tissue without the involvement of an anatomical obstacle. *Circ Res*. 1977;41:9-18.

16. Hou L, Deo M, Furspan P, Pandit SV, Mironov S, Auerbach DS, Gong Q, Zhou Z, Berenfeld O, Jalife J. A major role for HERG in determining frequency of reentry in neonatal rat ventricular myocyte monolayer. *Circ Res*. 2010;107:1503-1511.

17. Lim ZY, Maskara B, Aguel F, Emokpae R, Jr., Tung L. Spiral wave attachment to millimeter-sized obstacles. *Circulation*. 2006;114:2113-2121.

18. Baker LC, London B, Choi BR, Koren G, Salama G. Enhanced dispersion of repolarization and refractoriness in transgenic mouse hearts promotes reentrant ventricular tachycardia. *Circ Res*. 2000;86:396-407.

19. Chang MG, Zhang Y, Chang CY, Xu L, Emokpae R, Tung L, Marban E, Abraham MR. Spiral waves and reentry dynamics in an in vitro model of the healed infarct border zone. *Circ Res*. 2009;105:1062-1071.

20. Weiss JN, Garfinkel A, Karagueuzian HS, Chen PS, Qu Z. Early afterdepolarizations and cardiac arrhythmias. *Heart Rhythm*. 2010;7:1891-1899.

21. Sato D, Xie LH, Sovari AA, Tran DX, Morita N, Xie F, Karagueuzian H, Garfinkel A, Weiss JN, Qu Z. Synchronization of chaotic early afterdepolarizations in the genesis of cardiac arrhythmias. *Proc Natl Acad Sci U S A*. 2009;106:2983-2988.

22. Qin D, Zhang ZH, Caref EB, Boutjdir M, Jain P, El-Sherif N. Cellular and ionic basis of arrhythmias in postinfarction remodeled ventricular myocardium. *Circ Res*. 1996;79:461-473.

23. Stengl M, Ramakers C, Donker DW, Nabar A, Rybin AV, Spatjens RL, van der Nagel T, Wodzig WK, Sipido KR, Antoons G, Moorman AF, Vos MA, Volders PG. Temporal patterns of electrical remodeling in canine ventricular hypertrophy: focus on IKs downregulation and blunted beta-adrenergic activation. *Cardiovasc Res*. 2006;72:90-100.

24. Xie Y, Sato D, Garfinkel A, Qu Z, Weiss JN. So little source, so much sink: requirements for afterdepolarizations to propagate in tissue. *Biophys J*. 2010;99:1408-1415.

25. Liu J and Laurita KR. The mechanism of pause-induced torsade de pointes in long QT syndrome. *J Cardiovasc Electrophysiol*. 2005;16:981-987.

26. Spach MS and Dolber PC. Relating extracellular potentials and their derivatives to anisotropic propagation at a microscopic level in human cardiac muscle. Evidence for electrical uncoupling of side-to-side fiber connections with increasing age. *Circ Res*. 1986;58:356-371.

27. de Bakker JM, van Capelle FJ, Janse MJ, Tasseron S, Vermeulen JT, de JN, Lahpor JR. Slow conduction in the infarcted human heart. 'Zigzag' course of activation. *Circulation*. 1993;88:915-926.

28. Vasquez C, Mohandas P, Louie KL, Benamer N, Bapat AC, Morley GE. Enhanced fibroblast-myocyte interactions in response to cardiac injury. *Circ Res*. 2010;107:1011-1020.

29. Miragoli M, Salvarani N, Rohr S. Myofibroblasts induce ectopic activity in cardiac tissue. *Circ Res*. 2007;101:755-758.

30. Miragoli M, Gaudesius G, Rohr S. Electrotonic modulation of cardiac impulse conduction by myofibroblasts. *Circ Res*. 2006;98:801-810.

31. Zlochiver S, Munoz V, Vikstrom KL, Taffet SM, Berenfeld O, Jalife J. Electrotonic myofibroblast-to-myocyte coupling increases propensity to reentrant arrhythmias in two-dimensional cardiac monolayers. *Biophys J*. 2008;95:4469-4480.

32. Askar SF, Bingen BO, Swildens J, Ypey DL, van der Laarse A, Atsma DE, Zeppenfeld K, Schalij MJ, de Vries AA, Pijnappels DA. Connexin43 silencing in myofibroblasts prevents arrhythmias in myocardial cultures: role of maximal diastolic potential. *Cardiovasc Res*. 2012;93:434-444.

33. Pedrotty DM, Klinger RY, Kirkton RD, Bursac N. Cardiac fibroblast paracrine factors alter impulse conduction and ion channel expression of neonatal rat cardiomyocytes. *Cardiovasc Res*. 2009;83:688-697.

34. Danik SB, Liu F, Zhang J, Suk HJ, Morley GE, Fishman GI, Gutstein DE. Modulation of cardiac gap junction expression and arrhythmic susceptibility. *Circ Res*. 2004;95:1035-1041.

35. Peters NS, Green CR, Poole-Wilson PA, Severs NJ. Reduced content of connexin43 gap junctions in ventricular myocardium from hypertrophied and ischemic human hearts. *Circulation*. 1993;88:864-875.

36. Furukawa T and Kurokawa J. Potassium channel remodeling in cardiac hypertrophy. *J Mol Cell Cardiol*. 2006;41:753-761.

37. Zitron E, Gunth M, Scherer D, Kiesecker C, Kulzer M, Bloehs R, Scholz EP, Thomas D, Weidenhammer C, Kathofer S, Bauer A, Katus HA, Karle CA. Kir2.x inward rectifier potassium channels are differentially regulated by adrenergic alpha1A receptors. *J Mol Cell Cardiol*. 2008;44:84-94.

38. Zhang TT, Takimoto K, Stewart AF, Zhu C, Levitan ES. Independent regulation of cardiac Kv4.3 potassium channel expression by angiotensin II and phenylephrine. *Circ Res*. 2001;88:476-482.

39. Hoppe UC, Marban E, Johns DC. Molecular dissection of cardiac repolarization by in vivo Kv4.3 gene transfer. *J Clin Invest*. 2000;105:1077-1084.

40. Pijnappels DA, Schalij MJ, van Tuyn J, Ypey DL, de Vries AA, van der Wall EE, van der Laarse A, Atsma DE. Progressive increase in conduction velocity across human mesenchymal stem cells is mediated by enhanced electrical coupling. *Cardiovasc Res*. 2006;72:282-291.